Synthesis and Characterization of Dimensionally Ordered Semiconductor Nanowires within Mesoporous Silica

Nicholas R. B. Coleman, Niall O'Sullivan, Kevin M. Ryan, Timothy A. Crowley, M. A. Morris, Trevor R. Spalding, David C. Steytler,‡ and Justin D. Holmes*,†

Contribution from the Department of Chemistry and Supercritical Fluid Centre, University College Cork, Cork, Ireland, and School of Chemical Sciences, University of East Anglia, Norwich, NR4 7TJ, UK

Received March 15, 2001. Revised Manuscript Received May 9, 2001

Abstract: Semiconductor nanowires of silicon have been synthesized within the pores of mesoporous silica using a novel supercritical fluid solution-phase approach. Mesoporous silica, formed by the hydrolysis of tetramethoxysilane (TMOS) in the presence of a triblock copolymer surfactant, was employed for the nucleation and growth of quantum-confined nanowires. The filling of the silica mesopores with crystalline silicon and the anchoring of these nanowires to the sides of the pores were confirmed by several techniques including electron microscopy, powder X-ray diffraction, ^{29}Si magic angle spinning nuclear magnetic resonance, infrared spectroscopy, and X-ray fluorescence. Effectively, the silica matrix provides a means of producing a high density of stable, well-ordered arrays of semiconductor nanowires in a low dielectric medium. The ordered arrays of silicon nanowires also exhibited discrete electronic and photoluminescence transitions that could be exploited in a number of applications, including nanodevices and interconnects.

Introduction

Nanoscale structures of semiconductor wires are expected to play a vital role as materials for both interconnects and emerging future technologies because of their unique optical, electrical, and mechanical properties.[1,2] Several synthetic strategies have been developed for generating nanowires with diameters less than 10 nm and aspect ratios greater than 1000. Solution-phase methods, previously exploited for producing bulk quantities of semiconductor nanoparticles, have also been extended to the formation of nanowires. For example, Trentler et al.[3] successfully prepared indium phosphide wires by heating solutions of organometallic precursors. More recently, Holmes et al.[4] were able to control the structural orientation and hence optical properties of silicon nanowires using a supercritical solution-phase approach. Vapor−liquid−solid (VLS) growth methods using laser ablation techniques have also yielded semiconductor nanowires that have afforded an insight into their 1D optical and electronic properties.[5−8]

Even though the preparation of semiconductor nanowires in bulk quantities is now possible, unanswered questions relating to their processibility remain. A limiting step toward the development of nanotechnology is the templating of nanomaterials into useful electronic device architectures. Nanometer-wide channels of anodic aluminum oxide films,[9,10] polycarbonate track etched membranes,[11] and nanochannel array glasses[12] have previously been used as templates for nanowires of conductive polymers,[13] metals,[14] and semiconductors.[15] While these templating methods are useful, forming an ordered array of nanoscale channels is difficult and the channel dimensions are usually too large to engineer nanowires that exhibit quantum confinement effects.

Mesoporous solids[16−19] that contain unidirectional arrays of pores, typically 2−15 nm in diameter, running throughout the material have been successfully exploited as templates for semiconductor materials formed from the gas phase.[20−22] In particular, Leon et al.[20] reported the partial filling of MCM-41 mesoporous silica with germanium wires using vapor-phase epitaxy. In a similar approach Dag et al.[22] employed chemical

* To whom correspondence should be addresses: (phone) +353 (0)21 4903608; (fax) +353 (0)21 4274097; (e-mail) j.holmes@ucc.ie.

‡ University of East Anglia.

† Supercritical Fluid Centre, University College Cork.

(1) Brus, L. *J. Phys. Chem.* **1994**, *98*, 3575.
(2) Yeh, C.-Y.; Zhang, S. B.; Zunger, A. *Phys. Rev. B* **1994**, *50*, 14405.
(3) Trentler, T. J.; Goel, S. C.; Hickman, K. M.; Viano, A. M.; Chiang, M. Y.; Beatty, A. M.; Gibbons, P. C.; Buhro, W. E. *J. Am. Chem. Soc.* **1997**, *119*, 2172.
(4) Holmes, J. D.; Johnston, K. P.; Doty, R. C.; Korgel, B. A. *Science* **2000**, *287*, 1471.
(5) Morales, A. M.; Lieber, C. M. *Science* **1998**, *279*, 208.
(6) Wu, Y.; Yang, P. *Chem. Mater.* **2000**, *12*, 605.
(7) Duan, X.; Lieber, C. M. *J. Am. Chem. Soc.* **2000**, *122*, 188.
(8) Hu, J.; Odom, T. W.; Lieber, C. M. *Acc. Chem. Res.* **1999**, *32*, 435.
(9) Li, Y.; Xu, D.; Zhang, Q.; Chen, D.; Huang, F.; Xu, Y.; Guo, G.; Gu, Z. *Chem. Mater.* **1999**, *11*, 3433.
(10) Schmid, G.; Baumle, M.; Geerkens, M.; Heim, I.; Osemann, C.; Sawitowski, T. *Chem. Soc. Rev.* **1999**, *28*, 179.
(11) Schonenberger, C.; van der Zande, B. M. I.; Fokkink, L. G. J.; Henny, M.; Schmid, C.; Kruger, M.; Bachtold, A.; Huber, R.; Staufer, U. *J. Phys. Chem. B* **1997**, *101*, 5497.
(12) Nguyen, P. P.; Pearson, D. H.; Tonucci, R. J.; Babcock, K. *J. Electrochem. Soc.* **1998**, *145*, 247.
(13) Cepak, V. M.; Hulteen, J. C.; Che, G.; Jirage, K. B.; Lakshmi, B. B.; Fischer, E. R.; Martin, C. R. *Chem. Mater.* **1997**, *9*, 1065.
(14) Cepak, V. M.; Martin, C. R. *J. Phys. Chem. B* **1998**, *102*, 9985.
(15) Martin, C. R. *Science* **1994**, *266*, 1961.
(16) Kresage, C. T.; Leonwicz, M. E.; Roth, W. J.; Vartuli, J. C.; Beck, J. S. *Nature* **1992**, *359*, 710.
(17) Yu, C.; Yu, Y.; Zhao, D. *J. Chem. Soc., Chem. Commun.* **2000**, 575.
(18) Schmidt-Winkel, P.; Glinka, C. J.; Stucky, G. D. *Langmuir* **2000**, *16*, 356.
(19) Whitehead, A. H.; Elliott, J. M.; Owen, J. R.; Attard, G. S. *J. Chem. Soc., Chem. Commun.* **1999**, 331.
(20) Leon, R.; Margolese, D.; Stucky, G.; Petroff, P. M. *Phys. Rev. B* **1995**, *52*, R2285.
(21) Moller, K.; Bein, T. *Chem. Mater.* **1998**, *10*, 2950.
(22) Dag, O.; Ozin, G. A.; Yang, H.; Reber, C.; Bussiere, G. *Adv. Mater.* **1999**, *11*, 474.

10.1021/ja015833j CCC: $20.00
Published on Web 06/27/2001

vapor deposition (CVD) to deposit silicon nanocrystals within the pores of hexagonal mesoporous films. Certainly, these gas-phase methods have yielded high-quality semiconductor nanomaterials but the high temperatures, ca. 800 °C, or extensive reaction times, ca. 48 h, often required for successful nucleation and growth of the materials within the mesopores makes these techniques both costly and time-consuming.[20,22]

Recently, we reported the use of a novel supercritical fluid solution-phase approach to produce silicon nanowires within the pores of mesoporous silica.[23] The high-diffusivity[24] of the fluid enables the rapid transport of the silicon precursor into the mesopores of the silica thereby allowing swift nucleation and growth and reducing the reaction time for pore filling by at least an order of magnitude compared to CVD. Such a comprehensive filling of the mesopores with silicon nanowires was previously unobserved. In this paper, we describe in detail the use of a nonionic triblock copolymer surfactant to template the formation of ordered hexagonal silica mesoporous materials and the subsequent formation of silicon nanowires and nanorods within the walls of the silica matrix. Furthermore, the optical properties of the mesoporous silicon nanowires are compared to silicon nanowires grown from gold-seeded nanocrystals.[4]

Experimental Section

Preparation of Silicon Nanowires within Mesoporous Silica. Hexagonal mesoporous silica was prepared by a method based on one described by Attard et. al.,[25] i.e. the hydrolysis of tetramethoxysilane (TMOS) in the presence of a poly(ethylene oxide) (PEO)−polypropylene oxide (PPO) triblock copolymer surfactant ($PEO_{26}PPO_{39}PEO_{26}$)[17,18] (Synperonic P85 supplied by Uniquema, Belgium). In a typical synthesis Synperonic P85 (1 g) was dissolved in TMOS (1.8 g, 0.0118 mol) and added to an aqueous solution of HCl (1 g, 0.5 M). Methanol generated during the reaction was removed on a rotary film evaporator at 40 °C. The resulting viscous gel was left to condense at 40 °C for one week in a sealed flask. Calcination of the silica was carried out in air for 24 h at 450 °C. Any residual organic structure directing agent was then removed by flowing a 5% ozone stream over the dried inorganic oxide layer for 30 min.

Silicon nanowires were formed within the mesoporous silica (0.5 g) by degrading diphenylsilane (4.055 g, 0.022 mol) in a high-pressure reaction cell.[4] The high-pressure cell was attached, via a three-way valve, to a stainless steel high-pressure tube (∼21 mL) equipped with a stainless steel piston. An Isco high-pressure pump (Isco Instruments, PA) was used to pump carbon dioxide into the back of the piston and displace oxygen-free anhydrous hexane into the reaction cell to the desired pressure. The cell was placed in a tube furnace and heated to 500(±1) °C using a platinum resistance thermometer and temperature controller. The reaction proceeded at these conditions for 15 min. The mesoporous silica changed color from white to yellow to dark orange/red during the course of the reaction. The end product was homogeneous in appearance. No color change was observed in the absence of diphenylsilane. After the reaction had finished the contents of the cell were washed out with hexane. The relatively large (∼1 mm dimensions) particles of the dark orange/red mesoporous silica incorporating silicon collected from the reaction cell were washed in copious amounts of anhydrous hexane and ethanol. After each washing an aliquot of the supernatant was examined by gas-chromatography mass-spectrometry (GC-MS, Varian 2000 GC/MS/MS) to confirm the removal of any residual precursor and reaction intermediates formed during the course of the reaction.

Warning: The high pressures and temperatures used in these experiments and the volatile nature of the chemicals could potentially lead to fire or explosion. Suitable safety precautions should be taken into consideration including the use of a blast screen.

Preparation of Gold-Seeded Silicon Nanowires. Silicon nanowires were grown on gold nanocrystals as a substrate using a modification of the method published by Holmes et. al.[4] Under a nitrogen atmosphere, dodecanethiol-capped gold nanocrystals were dispersed in diphenylsilane with a Au:Si ratio of 0.1%, then loaded into the high-pressure cell (5 mL) and sealed under a nitrogen atmosphere. The cell was heated and pressurized as previously described.

Mesoporous Silica and Nanowire Characterization. Small-angle neutron scattering (SANS) measurements were performed on binary P85/D_2O systems and the resulting uncalcined and calcined mesoporous silicas from the same preparation. A detailed treatment of SANS theory is readily available in many textbooks.[26] Using D_2O gives good "contrast" in the scattering length density between the surfactant phase and the medium resulting in well-defined peaks. The SANS experiments were performed on the LOQ instrument at ISIS at the Rutherford Appleton Laboratory, UK. The samples were contained in flat quartz cells (1 mm sample thickness) sealed with Teflon stoppers. All SANS measurements were performed at 25 °C.

A JEOL 1200 EX electron microscope operating with an 80 kV accelerating voltage was used for transmission electron microscopy (TEM). Samples were redispersed in chloroform and a drop of the mixture was placed on a carbon-coated copper TEM grid. Powder X-ray diffraction (PXRD) profiles were recorded on a Philips 3710 PWD diffractometer, equipped with a Cu Kα radiation source and standard scintillation detector. Silicon magic angle spinning nuclear magnetic resonance (^{29}Si MAS NMR) spectra were obtained at room temperature using a Chemagnetics CMX Lite 300 MHz spectrometer. Cross-polarization was not used because of the exceptionally long relaxation times of the silicon nuclei, i.e. of the order of hours. Pulses of 30° with 4 s pulse width were used. Pulse delay times were varied in the range from 10 to 8000 s depending on the relaxation process. The delay times used were strongly dependent on the material studied suggesting that different relaxation mechanisms exist. Even at the delay times used, signal saturation was observed after a large number of scans for some of the samples studied. The gold-seeded silicon nanowires required the longest pulse delay times of approximately 6000−8000 s because of extremely slow relaxation processes. Delay times between 10 and 100 s were used for all the mesoporous silica materials. Samples were spun at 5 kHz. Chemical shifts are quoted relative to tetramethylsilane and referenced using tetramethoxysilane. An estimation of pore filling of the mesoporous silica with silicon was obtained by comparing the peak areas and peak shifts of the unfilled mesoporous silica samples directly to the filled materials. Note that these data were collected at several pulse delays so as to confirm that saturation was not affecting the relative intensity of the Si^0 and Si^{4+} signals.

The UV/visible spectra of the silica samples suspended in hexane were recorded on a Hewlett-Packard HP 8543 diode array spectrophotometer. Photoluminescence (PL) and photoluminescence excitation (PLE) spectra of the mesoporous silica samples suspended in hexane were recorded on a Perkin-Elmer LS 50 fluorescence spectrophotometer. Prior to dispersion in hexane the samples were ground into a fine powder. Diffuse reflectance attachments were used on both the UV/visible and fluorescence spectrometers to reduce scattering from the samples. The surface areas of the samples were measured using nitrogen BET isotherms at 77 K on a Micromeritics ASAP 2010 volumetric analyzer (Norcross, GA). Before the adsorption data were measured the samples were degassed for 12 h at 120 °C. Infrared spectra of the silica samples in a KBr matrix were recorded on a Bio-Rad FTS 3000 FTIR spectrophotometer. X-ray fluorescence (XRF) data were collected on an Oxford Instruments MDX 1080 spectrometer, equipped with a Rh source. Samples were pressed into self-supporting 4−7 mm thick disks using oxygen-free polyethylene as a binding medium. Samples were analyzed in a vacuum. The spectra were quantified with reference to various silica and zeolite materials. An accuracy of ±5% in Si:O stoichiometry was possible using these methods.

(23) Coleman, N. R. B.; Morris, M. A.; Spalding, T. R.; Holmes, J. D. *J. Am. Chem. Soc.* **2001**, *123*, 187.

(24) Clifford, T. *Fundamentals of Supercritical Fluids*; 1st ed.; Oxford University Press: New York, 1998.

(25) Attard, G. S.; C., G. J.; Goltner, C. G. *Nature* **1995**, *378*, 366. Goltner, C.; Berton, B.; Kramer, E.; Antonietti, M. *Adv. Mater.* **1999**, *11*, 395.

(26) Eastoe, J. *Small-Angle Neutron Scattering and Neutron Reflection*; Dickinson, E., Ed.; Blackie Academic & Professional: Glasgow, 1995; p 268.

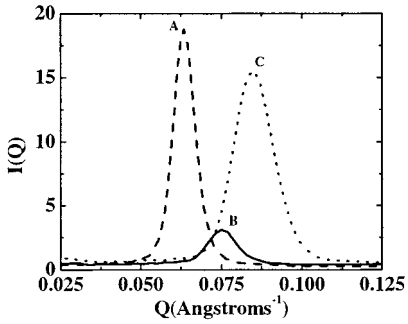

Figure 1. Small-angle neutron scattering (SANS) patterns for (a) P85/D_2O mixtures, (b) as-prepared uncalcined mesoporous silica, and (c) calcined mesoporous silica.

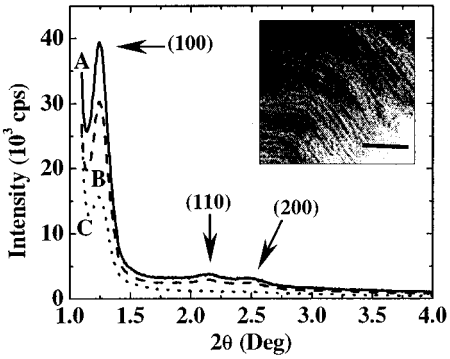

Figure 2. PXRD patterns of (a) as-synthesized calcined mesoporous silica prepared using $PEO_{26}PPO_{39}PEO_{26}$ triblock copolymer surfactant, (b) the same hexagonal mesoporous sample after exposure to hexane ($T = 500$ °C, $P = 375$ bar) for 15 min, and (c) mesoporous silica after silicon nanowire inclusion in the mesopores. The insert shows a "side-on" TEM image of the as-synthesized calcined mesoporous silica after incorporation of silicon through diphenylsilane decomposition (scale bar = 50 nm).

Results and Discussion

Stability of the Silica Mesopores. The use of triblock copolymer surfactants has been widely adopted in the synthesis of stable mesoporous silicas, e.g. SBA-15.[27,28] These mesoporous materials are typically synthesized using a surfactant concentration of between 1 and 10 wt %, with respect to water. The mesoporous silica samples synthesized in these experiments were prepared using a novel preparation in which a higher surfactant concentration, 50 wt % with respect to water, was used as a hexagonal template.[29] This preparation is similar to the liquid crystal templating method used by Attard et al.[25] to prepare mesoporous silicas from short chain ethylene oxide surfactants.

Figure 1a shows small-angle neutron scattering (SANS) data for the hexagonal liquid crystal phase formed using 50 wt % P85 surfactant, relative to D_2O, prior to silica condensation. Also shown are the SANS data for the mesoporous silica formed from the P85/D_2O mixture, before and after calcination at 450 °C (Figures 1b and 1c).

The modulus of the neutron momentum transfer (Q_{max}) for the surfactant mixture and the uncalcined and the calcined silica samples were determined as 0.0635, 0.0750, and 0.0850, respectively. From the measured Q_{max} values the hexagonal pore center-to-pore center distances were calculated to be 11.4 nm for the surfactant/D_2O sample, 9.6 nm for the uncalcined mesoporous silica, and 8.5 nm for the calcined silica material from the same preparation. The contraction of the hexagonal lattice upon silica condensation and drying, and again on calcination of the surfactant, is probably due to progressive silica condensation and physical relaxation of the silica framework as the surfactant and D_2O are removed.[30] The difference in the intensity of the scattering from each sample ($I(Q)$) is related to the difference between the scattering length densities of the sample and surrounding medium. For the surfactant/D_2O system there is good "contrast" between the two components producing an intense scattering peak. With the uncalcined silica sample the contrast between the silica sample containing the surfactant template and the medium (air) is poor resulting in a low-intensity SANS peak compared to the other samples (Figure 1c). Thus, at a concentration of 50 wt % the copolymer P85 adopts a hexagonal liquid crystal phase that is ideally suited for forming hexagonal mesoporous silicas with definite uniform pore dimensions.

Previously we reported[23] that three well-resolved peaks can be readily indexed to (100), (110), and (200) reflections for hexagonal mesoporous silica (Figure 2a).[27,31] The position of the intense (100) peak reflects a d spacing of 7.1 nm corresponding to a pore center-to-pore center distance of 8.2 nm, compared to a distance of 8.5 nm calculated from the SANS experiment.

Figure 2b shows the PXRD spectrum of the same mesoporous silica sample after 15 min exposure to hexane at 500 °C and 375 bar in a high-pressure reaction vessel. The position of the intense (100) peak did not change under the supercritical fluid reaction conditions. Reflections from the (110) and (200) planes are also still present. Clearly, the mesoporous silicas obtained using the P85 surfactant are sufficiently robust to withstand the supercritical reaction conditions used in the present experiments. We have also observed that hexagonal mesoporous silicas formed from other triblock surfactants, such as Pluronic P123 ($E_{20}P_{69}E_{20}$, supplied by BASF, UK), are also robust enough to withstand the extreme reaction conditions.

Mesoporous silicas have previously been shown to be stable to reaction temperatures of 800 °C[32] and pressures of 1.2×10^5 bar,[33] but to our knowledge the stability of mesoporous silica under both high temperature and pressure conditions in a supercritical fluid has not been demonstrated.

Silicon Inclusion: Nanowire Formation. Figure 2c shows the low-angle PXRD pattern obtained after inclusion of silicon in the mesoporous silica. A pore pore-to-pore distance of 8.3 nm was observed for the mesoporous silica matrix after silicon inclusion. The reduced intensity of the (100) peak and the absence of the (110) and (200) peaks after inclusion was noted. This effect probably arises from the presence of silicon in the mesopores, which results in an increased residual strain on the silica walls.[34] This conclusion is based on ^{29}Si MAS NMR data (Figure 3), which illustrate that there are only small changes in the width of the Q_4 or $Si(OSi)_4$ peak after silicon inclusion. [3]The complete extinction of the PXRD reflections has previously

(27) Zhao, D.; Sun, J.; Li, Q.; Stucky, G. D. *Chem. Mater.* **2000**, *12*, 275.
(28) Zhao, D. Y.; Huo, Q. S.; Feng, J. L.; Chmelka, B. F.; Stucky, G. D. *J. Am. Chem. Soc.* **1998**, *120*, 6024.
(29) Chu, B.; Zhou, Z. In *Nonionic Surfactants: Polyoxyalkylene Block Copolymers*; Nace, V. M., Ed.; Surface Science Series, Vol. 60; Marcel Dekker: New York, 1996.
(30) Edler, K. J.; Reynolds, P. A.; White, J. W. *J. Phys. Chem. B* **1998**, 3676.
(31) Junges, U.; Jacobs, W.; Voight-Martin, I.; Krutzsch, B.; Schuth, F. *J. Chem. Soc., Chem. Commun.* **1995**, 2283.
(32) Walker, V. J.; Morey, M.; Carlsson, H.; Davidson, A.; Stucky, G. D.; Butler, A. *J. Am. Chem. Soc.* **1997**, *119*, 6921.
(33) Wu, J.; Liu, X.; Tolbert, S. H. *J. Phys. Chem. B* **2000**, *104*, 11837.
(34) Marler, B.; Oberhagemann, U.; Vortmann, S.; Gies, H. *Microporous Mater.* **1996**, *6*, 375.

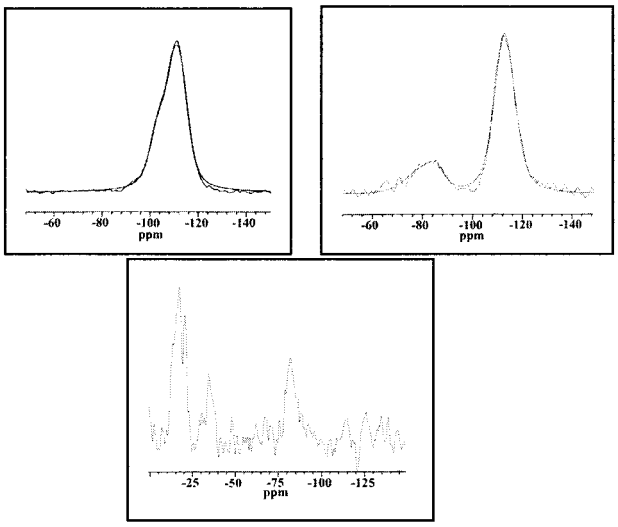

Figure 3. ^{29}Si MAS NMR spectra of (a, top left) a mesoporous silica sample before and (b, top right) after silicon inclusion and (c, bottom) silicon nanowires grown from gold nanocrystals.

been reported upon inclusion of sorbates, such as bromoform, in boron-containing MCM-41 materials.[34] The loss of the (110) and (200) peaks could also be interpreted as resulting from a decreased correlation length due to the increased disorder in the material after nanowire inclusion. However, if there had been any significant structural changes in the mesoporous structure then large changes in the width and position of the Q_4 peak should have been observed. A "side-on" view of the mesoporous silica incorporating crystalline silicon is shown as an insert in Figure 2 and is further evidence for the inclusion of silicon within the mesopores.

Panels a and b in Figure 3 display ^{29}Si MAS NMR spectra of a mesoporous silica sample before and after silicon inclusion, respectively.

Prior to silicon inclusion two principal features are observed, as previously reported.[23] A peak at −111.4 ppm is assigned to the silica matrix (Q_4 or $Si(OSi)_4$ linkages) and a second feature between −103.4 and −106 ppm is due to silica species at the surface of the pore, i.e. Q_3 or $Si(OSi)_3(OH)$.[22,35] A smaller feature apparent at −92.4 ppm we have assigned to Q_2 or $Si(OSi)_2(OH)_2$ seen typically at kink sites in the wall.[22] Upon inclusion of silicon, in the mesoporous matrix, a peak appears at −80 ppm due to the presence of elemental silicon. Curve fitting of the peak at −80 ppm resolved the peak into two features, one at −80.8 ppm due to crystalline silicon (Si_4Si) and one at −88 ppm due to silicon atoms attached to the surface of the intrachannel silica walls ($Si(OSi)_3$(wall)−O−Si(wire)). Inclusion of the silicon also results in complete removal of the pore related features at −103.4 and −92.4 ppm and infers that the silicon nanowires are anchored to the surface of the mesoporous walls and pore-filling has been achieved.

The ^{29}Si MAS NMR spectrum of silicon nanowires grown on colloidal gold nanoparticles as nucleation seeds[4] exhibited a series of features from −15 to −82.5 ppm, Figure 3c. The peaks below −80 ppm can possibly be assigned to low coordination atoms on the surface of the nanowires (Si(surface)). The absence of these surface features in the spectra of the mesoporous templated silicon nanowires and the appearance of the −88 ppm peak (Si_4Si) suggests that the surfaces of the mesoporous nanowires have been modified possibly as a result of the wire anchoring to the silica walls.

(35) Steel, A.; Carr, S. W.; Anderson, M. W. *Chem. Mater.* **1995**, *7*, 1829.

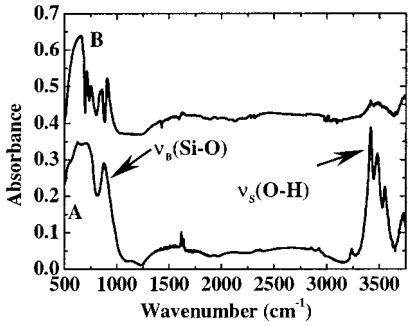

Figure 4. FTIR spectra of (a) as-synthesized calcined mesoporous silica before and (b) after silicon inclusion.

The ^{29}Si cross-polarization MAS NMR experiments were not recorded for the mesoporous and gold-grown silicon nanowire samples due to the long relaxation times (T_1) of the nuclei involved. For the silicon nanowires seeded from gold nanocrystals T_1 was between 6k and 8k s depending on the method of preparation, in contrast to the T_1 delay times for mesoporous silicon nanowires between 15 and 60 s. For none of the gold-grown silicon nanowire samples studied did we observe T_1 relaxation times similar to those observed for the mesoporous silicon nanowires. The lower relaxation times for the mesoporous silicon nanowires, compared to the gold-seeded wires, further suggests that the nanowires themselves are in direct contact with the silica walls as inferred by the peak at −88 ppm.

Figure 4 shows the FTIR spectra of calcined mesoporous silica (a) before and (b) after silicon inclusion. The silanol vibrational modes, an O−H stretch, ν_S(O−H), at 3700−3200 cm^{-1} and an Si−O bending mode, ν_B(Si−O), at 874 cm^{-1}, are present in the mesoporous silica before silicon inclusion.[22,36]

After silicon nanowire formation the Si−O bending mode at 874 cm^{-1} almost completely disappears and there is a significant reduction of the O−H stretching mode probably due to the anchoring of the silicon nanowire to the mesoporous walls.[22] Dag et al.[22] previously reported the presence of vibrational modes between 2300 and 2100 cm^{-1} due to Si−H stretching modes, upon forming 1 nm silicon clusters in orientated hexagonal mesoporous films. The absence of Si−H stretches is consistent with filling of the mesopores with silicon nanowires. Also, the absence of Si−Ph stretching bands between 3080 and 3030 cm^{-1} indicates complete degradation of the diphenylsilane precursor to silicon within the mesopores.

Quantitative evidence for comprehensive filling of the mesopores with silicon nanowires comes from ^{29}Si MAS NMR, X-ray fluorescence (XRF) spectroscopy, and nitrogen adsorption isotherm data. The ^{29}Si MAS NMR (Figure 3) revealed that the volume ratio of $Si:SiO_2$ in the mesoporous sample was approximately 2.9 to 3.2:1, which correlates to about 80−90% of the mesopores being filled with silicon. This $Si:SiO_2$ ratio was estimated using densities for silicon and silica of 2.33 and 2.20 g cm^{-3}, respectively. Confirmation of the extent to which the pores were filled was obtained from XRF measurements. For the mesoporous silica a Si:O ratio of 1:1.96 was obtained. Upon inclusion of the silicon nanowires in the mesopores the Si:O ratio fell to 1:1.01, suggesting that approximately 95% of the pores are filled with silicon, which is in agreement with the NMR data. Also, nitrogen adsorption isotherm data for calcined mesoporous silica exhibited a high surface area of ∼1045 m^2

(36) Pretsch, E.; Clerc, T.; Seibl, J.; Simon, W. *Tables of Spectral Data for Structure Determination of Organic Compounds*: Springer-Verlag: Berlin, 1942. Socrates, G. *Infrared Characteristic Group Frequencies Tables and Charts*; John Wiley & Sons: New York, 1994.

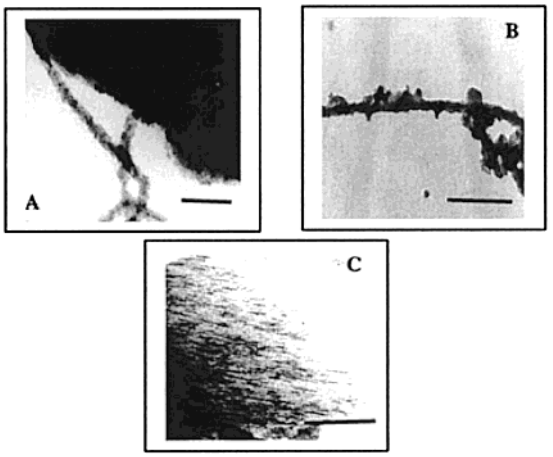

Figure 5. TEM images of (a) a silicon nanowire growing from the surface of a mesoporous silica surface (scale bar = 200 nm), (b) a silicon nanowire growth from the surface of a gold-seeded nanoparticle (scale bar = 20 nm), and (c) "side on" view of partially filled mesopores (scale bar = 400 nm).

g^{-1}. Upon inclusion of the silicon in the mesopores the surface area decreased to ~72 m^2 g^{-1}, supporting the hypothesis that the pores of the silica matrix are filled.

The Effect of Precursor Concentration. With diphenylsilane concentrations in excess of the concentration needed to fill the pores (>0.022 mol for 0.5 g of mesoporous silica), "whiskers" of silicon were observed protruding from the mesoporous silica surface (Figure 5a). The silicon "whiskers" were up to 4 μm in length and between 50 and 100 nm in diameter and therefore considerably larger in diameter than the size of the individual mesopores. Due to the low resolution of the TEM, and poor contrast of the sample, we could not make any further conclusions about, for example, if these whiskers were composed of smaller bundles of nanowires with dimensions comparable to the pore diameter of the silica mesopores, i.e. 5 nm. At high reactant concentrations it appears that the mesopores can act as sites for surface whisker growth. For comparison, Figure 5b shows a TEM of silicon nanowires grown from gold-seeded nanocrystals.[4]

At diphenylsilane loadings below 0.022 mol, nanoparticles and nanorods of silicon, between 10 and 200 nm in length, were observed within the pores of the silica matrix. Figure 5c shows a TEM image of silicon nanorods, up to 150 nm in length, formed inside the pores of a mesoporous silica matrix at a precursor concentration of 0.011 mol. Hence, the formation of micron length mesoporous nanowires of silicon possibly occurs through the initial formation of nanoparticles within the mesopores and the subsequent nucleation and growth of these nanocrystals into nanorods and then nanowires. Control over the precursor loading is therefore essential to achieve comprehensive filling of the mesopores.

The Mechanism of Silicon Nanowire Formation. The formation of the mesoporous silicon nanowires from diphenylsilane is clearly a complex process. At present it is not possible to define all of the intermediates that may be involved. However, taking into account the extreme reaction conditions and, most notably, the relatively high reaction temperature, it is probable that silicon-centered radical species are involved. It is well established in the literature that both γ-irradiation[37,38] and photolysis reactions[39−41] of organosilane derivatives $R_nSiH_{(4-n)}$

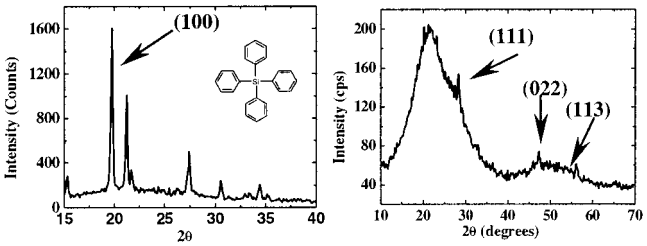

Figure 6. High-angle PXRD patterns for (a) tetraphenylsilane formed by the decomposition of diphenylsilane at 300 °C and 375 bar in the presence of mesoporous silica and (b) mesoporous silicon nanowires formed at 500 °C and 375 bar.

proceed via the initial formation of three-coordinate silicon-centered radical intermediates. Even though the Si−H and Si−C bond dissociation energies are expected to be similar at ca. 335 to 355 kJ mol^{-1} depending on the particular species involved, the evidence from kinetic studies is that Si−H bonds are broken in preference to Si−Ph bonds and the favored radicals are those retaining phenyl groups.[37,39] In this respect it is noteworthy that tetraphenylsilane is a product when diphenylsilane is reacted at 300 °C as shown in the PXRD pattern in Figure 6a.

However, to form silicon, it is necessary to remove all phenyl and hydride ligands from diphenylsilane. Gas chromatography−mass spectrometry (GC-MS) was used to ascertain some of the reaction intermediates formed during the decomposition of diphenylsilane to silicon. Benzene was detected by GC-MS in the hexane and ethanol washings of all reaction samples along with small amounts of several high molecular weight cyclic decomposition products, e.g. $Ph_3Si(Ph)Ph$ and $Ph_3Si(Ph)Ph$. Several organosilane species, in particular Ph_3SiH and $PhSiH_3$, were present in the supernatant when the samples were washed in anhydrous hexane only. When anhydrous ethanol was used instead of hexane to extract the intermediates, ethoxy silane species such as $Ph_3SiOC_2H_5$ and $PhSi(OC_2H_5)_3$ were detected in addition to the organosilane species observed in hexane. At reaction temperatures of 500 °C and reaction times in excess of 15 min no tetraphenylsilane was detected in any final washed or dried samples.

On the basis of the GC-MS results we suggest that one pathway for the formation of crystalline silicon possibly occurs through a rearrangement-type decomposition reaction as proposed by Levy and Coutant,[42] as shown below in reaction 1, resulting in the subsequent elimination of benzene (reactions 2 and 3):

$$2((Ph)_2SiH_2) \rightarrow Ph_3SiH + PhSiH_3 \quad (1)$$

$$PhSiH_3 \rightarrow Ph(H_2)Si: + C_6H_6 \quad (2)$$

$$Ph(H_2)Si: \rightarrow Si + C_6H_6 \quad (3)$$

The silicon atoms produced by reactions 2 and 3 would not be "stabilized" as was the case when a similar reaction was carried out in *n*-octanol[43] and would readily react with both sides of the mesoporous silica and with other silicon atoms. It is also possible that two phenylsilylene radicals may dimerize affording Ph(H)Si═Si(H)Ph although this species was not detected by GC-MS. This compound would have a silicon−silicon double

(37) Rhodes, C. J. *J. Chem. Soc., Perkin Trans.* **1992**, 1475.
(38) Seki, S.; Cromack, K. R.; Trifunac, A. D.; Yoshida, Y.; Tagawa, S.; Asai, K.; Ishigure, K. *J. Phys. Chem B* **1998**, *102*, 8367.
(39) Chatgilialoglu, C. *Chem. Rev.* **1995**, *95*, 1229.
(40) Sluggett, G. W.; Leigh, W. J. *Organometallics* **1992**, *11*, 3731.
(41) Kerst, C.; Potzinger, P. *J. Chem. Soc., Faraday Trans.* **1997**, 1071.
(42) Levy, A.; Coutant, R. W. *J. Organomet. Chem.* **1966**, *6*, 421 and references therein.
(43) Holmes, J. D.; Ziegler, K. J.; Johnston, K. P.; Doty, R. C.; Korgel, B. A *J. Am. Chem. Soc.* **2001**, *123*, 3743.

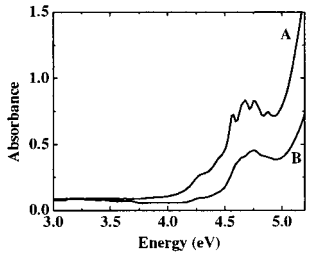

Figure 7. Uv/visible absorbance spectrum of (a) non-ozonized mesoporous silica loaded with crystalline silicon[23] and (b) ozonized mesoporous silica loaded with crystalline silicon.

bond of similar strength to the Si−H and Si−C bonds. Further reactions leading to the build up of silicon could be via the loss of hydride or benzene.

The purity and crystallinity of the mesoporous silicon nanowires was confirmed by PXRD at high angles (Figure 6b). The relatively sharp peaks in the PXRD pattern can be indexed to a diamond structure of silicon with a lattice constant $a = 0.543$ nm, which is in excellent agreement with literature values for silicon.[44] Due to the small dimensions of the silicon nanowires the sharp (111), (022), and (113) reflections, shown in Figure 6b, sit on broad diffraction peaks, approximately 2.0° in width. The Scherrer equation suggests that such a peak width corresponds to a crystallite size of 4.3 nm in one direction, which is close to the diameter of the mesopores. The extremely broad peaks (>20°) shown in Figure 6b are simple due to amorphous type scattering from the host matrix. Consequently, these results highlight the importance of reaction temperature on silicon nanowire formation. We are currently studying further the mechanism of silicon nanowire formation within the mesoporous systems.

Optical Properties of the Silicon Nanowires: UV/Visible. Previously we reported that silicon nanowires formed within mesoporous silica possessed similar optical properties to silicon nanowires seeded from gold nanocrystals, as shown in Figure 7a.[23] We also suggested that an absorption peak centered at 4.25 eV arises from absorption due to the mesoporous solid and residual precursor. Since those data were reported we have found that ozonolysis of the mesoporous silca after calcination results in almost complete removal of any residual organic template. The UV/visible absorption spectrum of silicon nanowires grown within ozonized mesoporous silica is shown in Figure 7b.

Examination of Figure 7a reveals that a peak previously observed to be centered at 4.25 eV arising from absorption due to the silica matrix has almost completely disappeared in the ozonized mesoporous silica sample (Figure 7b). Peaks centered at 4.7 eV, indicative of the L → L transition[45] previously reported for (100) orientated silicon nanowires,[14] are still present in Figure 7b but exhibit much weaker discrete absorbance features compared to Figure 7a. Consequently, the spectrum shown in Figure 7a may contain some residual precursor which can be readily removed using appropriate solvents (see Experimental Section).

Photoluminescence. Figure 8a shows the photoluminescence emission (PL) spectra of mesoporous silicon nanowires and 4−5 nm diameter silicon nanowires grown from colloidal gold nanocrystals, at an excitation energy of 4.68 eV.

At this energy both the mesoporous silicon nanowires and the gold-seeded wires exhibit a PL peak at 3.85 eV that is similar

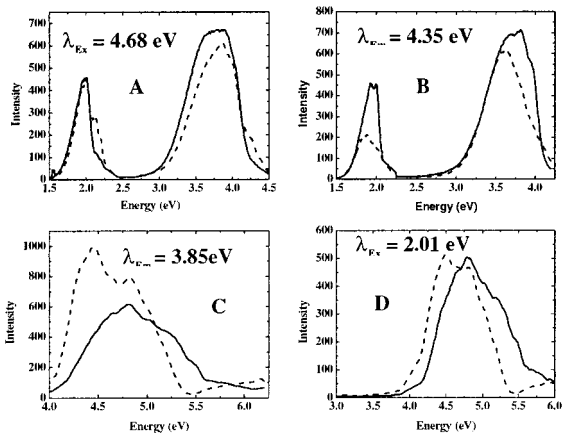

Figure 8. Photoluminescence (PL) spectra of mesoporous silica loaded with silicon nanowires (—) and silicon nanowires grown from gold nanocrystals (- - -) dispersed in hexane at excitation energies of (a) 4.68 and (b) 4.35 eV. Photoluminescence excitation (PLE) spectra of the same mesoporous silicon (—) and gold seeded nanowires (- - -) at emission energies of (c) 3.85 and (d) 2.01 eV.

to a value of 3.75 eV previously reported for (100) orientated silicon nanowires seeded from gold colloids.[4] A broad peak, centered at 2.01 eV, is also revealed in Figure 8a for both samples. This lower energy transition probably results from surface effects due to surrounding oxide layers of the nanowires.[46,47]

For both PL transitions the peaks of the mesoporous silicon nanowires are considerably more featureless than the peaks from the gold-grown nanowires and may be a consequence of binding of the mesoporous nanowires to the cell walls. Furthermore, the PL peak profiles and intensities appear to depend on the excitation energy (Figure 8b). As the excitation energy is decreased from 4.68 to 4.35 eV, the PL peak at 3.85 eV sharpens and the intensity of the PL peak at 2.01 eV decreases in intensity relative to the high-energy emission band, from an intensity ratio of 2:3 to 1:3. These profile and intensity changes were not observed with the gold-seeded nanowires and may be a consequence of interactions of the mesoporous silicon wires with the silica walls. Furthermore, unlike the gold-seeded nanowires of silicon whose PL is completely quenched over a period of between 1 and 2 weeks, the mesoporous silicon nanowires still exhibit PL after a period of 6 months.

The photoluminescence excitation (PLE) spectra of the mesoporous silicon and gold-grown silicon nanowires are shown in Figure 8c,d. The PLE of the silicon mesowires is slightly shifted in comparison to the gold-seeded nanowires at emission energies of 3.85 and 2.01 eV. The difference in the spectra may be due to quantum confinement effects caused by differences in the average diameters and aspect ratios of the two samples.

Conclusion

A novel supercritical fluid solution-phase technique has been utilized to fill the 5 nm diameter pores of hexagonal mesoporous silica, prepared using a contemporary surfactant templating method, with quantum-confined silicon nanowires. The low viscosity[24] of the supercritical fluid phase enables rapid diffusion of reactant precursor into the pores of the silica matrix where nucleation and growth on the pore walls occurs as confirmed by ^{29}Si MAS NMR and FTIR. Unlike CVD techniques where

(44) *JCPDS International Centre for Diffraction Data*; Powder Diffraction file 27-1402; 0.542 nm; 1984.

(45) Hu, J.; Ouyang, M.; Yang, P.; Lieber, C. M. *Nature* **1999**, *399*, 48−51.

(46) Lauerhaas, J. M.; Sailor, M. J. *Science* **1993**, *261*, 1567.

(47) Wolkin, M. V.; Jorne, J.; Fauchet, P. M.; Allan, G.; Delerue, C. *Phys. Rev. Lett.* **1999**, *82*, 197.

the deposited material grows in almost all directions, promoting the growth of solid material across the tops of the pores in the substrate and subsequent blocking of the pores, with this novel supercritical fluid method this is not observed. Furthermore, the discrete transitions observed in the UV−visible absorption and PL spectra suggest that the mesoporous nanowires possess quantum confinement effects that could be exploited in a number of applications, including nanodevices and interconnects. The high packing density of the silicon "mesowires" in the silica matrix makes them ideally suited for the formation of quantum structures.

Acknowledgment. We acknowledge financial support from the HEA Ireland Third Level Institution Grant and funding from Enterprise Ireland and Intel (Ireland). The support of the Dr. W. J. Reville and the Electron Microscopy Unit at UCC is also acknowledged. The authors are grateful for equipment support from Mitsui-Denman (Ireland) and DCU. A big thanks to Dr. L. Thuener for his time and help with GC-MS analysis. Thanks to Drs S. E. Lawrence and W. C. Mackrodt for useful discussions.

JA015833J